EVALUATION OF FLUTTER ANALYSES IN THE CONTEXT OF NEW CONCEPTS OF PRELIMINARY AIRCRAFT DESIGN

J.Rieke, W.Heinze, P.Horst
Institute of Aircraft Design and Lightweight Structures (IFL), TU-Braunschweig
Hermann-Blenk-Str. 35, 38104 Braunschweig, Germany
J.Schwochow
Institute of Aeroelastics, DLR-Göttingen
Bunsenstr.10 , 37073 Göttingen, Germany

ABSTRACT

The process chain of the aeroelastic flutter analysis for new aircraft configurations is presented in the context of the preliminary aircraft design and optimisation program PrADO of the IFL. Therefore a recalculated Fairchild Dornier 728JET is used as an example.

The different software modules used in this process chain are described together with the models, which are needed for the computation: PrADO is used to calculate a fully converged aircraft design by an iterative process. As eigen frequencies and eigen modes of the aircraft structure are used by flutter analysis, a structural model for modal analyses with MSC.NASTRAN® is generated by a PrADO sub module and transformed into the NASTRAN® bulkdata format. With geometry information of PrADO database a ZAERO®[1] model is created to perform automated evaluation of flutter proneness.

The results of the flutter analysis of the FD 728JET, performed at Fairchild Dornier (cp. [1]), are compared to the results of the PrADO design. The differences between both are detailed. Further a modified PrADO 728JET with winglets is compared to the baseline design.

NOTATION

ϕ	reduced frequency domain potential
ϕ_0	steady potential
ω	harmonic oscillation frequency
Φ	total velocity potential
Ψ	acceleration potential
a_∞	upstream sonic velocity
g	aerodynamic damping
i	negative root
k	reduced frequency
p	non dimensional Laplace parameter
q_∞	dynamic pressure
t	time
L	reference length
V	velocity of undisturbed flow
V_{EAS}	equivalent air speed
V_{TAS}	true air speed
$\{\boldsymbol{h}\}$	structural deformation vector at aerod. boxes
$\{\boldsymbol{q}\}$	generalised coordinates
$\{\boldsymbol{x}\}$	structural deformation vector at FE-nodes
$\{\boldsymbol{F}_a\}$	resultant aerod. forces at FE-nodes
$\{\boldsymbol{F}_h\}$	resultant aerod. forces at aerod. boxes due to $\{\boldsymbol{h}\}$
$[\boldsymbol{AIC}]$	matrix of aerodynamic influence coefficients
$[\boldsymbol{G}]$	spline matrix
$[\boldsymbol{K}]$	generalised stiffness matrix
$[\boldsymbol{M}]$	generalised mass matrix
$[\boldsymbol{Q}]$	generalised aerodynamic force matrix

Indices

tt	second partial derivation to t
xt	partial derivation to x and t
xx	second partial derivation to x
yy	second partial derivation to y
zz	second partial derivation to z

1. MOTIVATION

With the objective to design more and more economical aircraft the knowledge of the aeroelastic behaviour in the preliminary design phase gets an important role, because here, already during the concept level, designs must be benchmarked against each other without great efforts of calculation time. Thus it can be prevented, that at the time of the detail design phase subsequent changes have to be introduced, which mean losses in the economy of the resulting aircraft design.

Whereas therefore static aeroelastic analyses currently belong to the standard procedure in preliminary design, a corresponding, automatically running process for the first estimation of the critical flutter speed does not exist. Such a method enables the designer to quantify the sensitivities (modification of the configuration, e.g. change of wing sweep) of the flutter behaviour.

Against this background a process (FIG 1.) has been developed and tested on a known aircraft concept in collaboration with our partners at the German Aerospace Centre (DLR, Institute of Aeroelastics).

2. PROCESS CHAIN

FIG. 1 shows the modular process with the implemented software tools. To understand the procedure it is necessary to explain the involved modules in detail. The procedure is described in the following subchapters.

[1] ZAERO® is a toolkit by ZONA Technology Inc. for solving aeroelastic problems.

2.1. Preliminary Aircraft Design and Optimisation Tool – PrADO

PrADO is a multidisciplinary design and optimisation tool containing a parametric data structure. PrADO has been developed at the Institute of Aircraft Design and Lightweight Structures (IFL) for estimation of all aircraft aspects in the preliminary phase (cp. Heinze [2]). It provides the core for the described flutter calculation process and delivers the input data for other modules in the flutter process. To cover the multidisciplinary approach, PrADO is subdivided into several modules which represent single design disciplines.

2.1.1. PrADO Design Process

Before a calculation with PrADO can be started, an input file is required which contains data from a zero level aircraft design (e.g. ranges, transport missions, configuration, global geometric dimensions, …). These requirements are interpreted in the first module and are distributed into object ordered data bases. All modules use these data bases to read and store computed results.

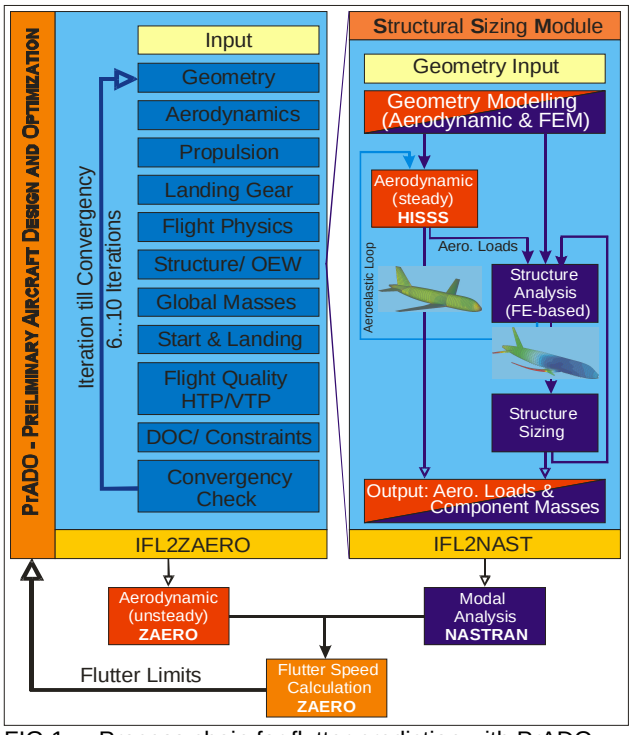

FIG 1. Process chain for flutter prediction with PrADO

The iterative aircraft design process (cp. FIG 1.) starts with the geometry module, which analyses the parametric, geometric input data and calculates the missing data to describe the aerodynamic surface, the structural design and interior of all aircraft components.

In the aerodynamics module the aerodynamic data field/ characteristics for the different flight and loading cases are calculated for the whole configuration. For this purpose different types of steady aerodynamic codes are available (e.g. lifting line code: Lifting Line [3], panel code: HISSS (EADS-M, [4])). The resulting properties are necessary for flight simulation to predict performance, control and stability properties (flight physics, start & landing, HTP/VTP flight quality modules).

The propulsion module computes the engine characteristics, which are needed besides the aerodynamic characteristics to evaluate the flight physics of the aircraft configuration.

In the landing gear module the **l**oad **c**lassification **n**umber (LCN), the load factor and the sizing are performed by handbook methods (cp. [2]).

The **o**perational **e**mpty **w**eight (OEW) is computed by the sizing module, which is described in the next subchapter 2.1.2. and is used by the following module where the global masses are composed.

At last the **d**irect **o**peration **c**osts (DOC) are computed and constraints are checked for convergence. If the check of the observed parameters is negative, a new iteration loop is started until convergence is reached.

2.1.2. PrADO: Structural Sizing Module

The module in which PrADO calculates the OEW mass is called the **S**tructural **S**izing **M**odule (SSM) and has been developed by [5]. Its primary function is the computation of the structural masses of the primary aircraft structure: fuselage, wing, **h**orizontal **t**ail **p**lane (HTP) and **v**ertical **t**ail **p**lane (VTP).

Corresponding to FIG. 1, the **f**inite **e**lement **m**ethod (FEM) is used for the sizing with different load cases, which are specified by manoeuvre and gust flight envelope corner points. The loads therefore are derived from a steady aerodynamic calculation with HISSS (cp. [5]) and compensated by inertia forces (payload, secondary masses).

The HISSS calculation needs a geometrical description of the aerodynamic shape, which is provided by a submodule called **m**ulti **m**odel **g**enerator (MMG). During the first step the MMG generates a NURBS [6] splined surface of the aircraft surfaces, based on the PrADO geometry description. Corner points for the aerodynamic panels are extracted from the NURBS geometry and stored in the HISSS mesh input file format.

The structural model is composed in a similar way. The location of e.g. the wing box or the fuselage frames is determined be the PrADO database and the precise node location can be interpolated from the NURBS description. In this way the nodes and elements are built up for all primary structure parts. The property entries of the FE-model are also generated by the MMG and are written to a special data base.

The sizing process of SSM consists of the sizing routine itself, the FE pre-processor, the FE solver and the FE post-processor, which are called step by step by the sizing

process in a loop. In the pre-processing part the resulting pressure distribution (c_p) from the aerodynamic calculation (rigid mesh) is transferred to discrete loads on the FE-model nodes (for detail see [5]). With this data set the implemented FE-solver [5] can calculate the von Mises (v.M.) stresses for every element. The v.M. stresses are used to size the model (increasing wall thicknesses and section parameters) by the principia of fully stressed design [5]. The iterative sizing process stops, if the mass change is lower than a limit, or a fixed number of steps are reached. Finally the post-processor calculates the masses of the single components listed before.

It should be mentioned that it is possible to size the model also as a flexible structure. Therefore every FE step an aerodynamic calculation with deformed mesh is performed until the aeroelastic equilibrium is fulfilled (see FIG. 1). This procedure highly increases the calculation time.

2.1.3. IFL2NAST

IFL2NAST is basically an export filter to convert the internal PrADO/ SSM FE data to the format of the commercial FE solver MSC.NASTRAN®.

There are two options for exporting data sets into MSC.NASTRAN® input files. With the first option all loads, boundary conditions and sized FE data are copied one-to-one into the MSC.NASTRAN® format and the original SSM load cases can be recalculated with MSC.NASTRAN® or read into a pre-/ post-processor such as MSC.PATRAN®.

With the second option only the FE data (i.e. nodes, elements and properties) are exported for modal analyses. As only one half of the symmetric aircraft is under investigation to reduce computational time, one load case includes symmetric **b**oundary **c**onditions (BC), the second includes anti-symmetric boundary conditions. Both resulting sets of eigen frequencies and eigen modes are a necessary input for the flutter calculation with ZAERO®.

2.1.4. IFL2ZAERO

IFL2ZAERO is also an export filter which converts the PrADO geometry definition into the ZAERO aerodynamic panel description. In addition to the load cases for ZAERO (altitude/ density, Mach number, BC, payload and fuel weight distribution), node lists for spline interpolation of the structure and output file requests are generated. The output of IFL2ZAERO is a set of input files for ZAERO, which can be started without additional manual input.

2.2. MSC.NASTRAN®

MSC.NASTRAN® is used as the standard FE solver for the modal analyses (solution 103). The input data set from IFL2NAST can be used directly for computation. The results in terms of the f06 output can be read in by ZAERO, which needs the eigen modes, frequencies and generalised masses for the flutter calculation.

2.3. ZAERO

ZAERO® by ZONA Technology is an aeroelastic toolkit for simulating all kind of aeroelastic design and analysis problems [7]. Here the basic modules are used to perform flutter calculations at subsonic speed.

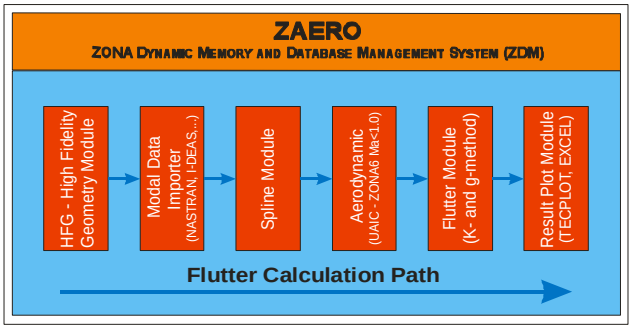

FIG 2. ZAERO – Modules used for Flutter Calculation

The process chain is shown in FIG 2. In the High Fidelity Geometry Module (HFG), the geometry given in the input file is transformed into the panel mesh for the unsteady aerodynamic calculation. The next step is to read in the results of the modal analyses, which are created by MSC.NASTRAN® and saved in the f06 files. For every component a structural spline has to be interpolated from the eigenmodes of the modal analyses. In the following module the unified **a**erodynamic **i**nfluence **c**oefficients matrix (AIC) is calculated by the subsonic unsteady aerodynamic module ZONA6® [8]. By multiplying the AIC with downwash resulting from harmonic oscillation of the eigenmodes the generalized aerodynamic loads can be calculated for different reduced frequencies.

The flutter solver evaluates the equations of motion in generalized form for frequencies and damping coefficients within a given flight velocity range. The results (damping versus velocity and frequency versus velocity diagrams) can be converted for visualisation into e.g. the TECPLOT® format.

2.3.1. Unsteady Aerodynamics

The calculation of the AIC matrix for subsonic speeds (ZONA6) is based on the unsteady three dimensional linearized potential equations for small disturbances (equation (1), compare [8]). The numerical solution of this equation is done by a panel method.

(1) $$(1-Ma_\infty^2)\Phi_{xx}+\Phi_{yy}+\Phi_{zz}-\frac{1}{a_\infty^2}\Phi_{tt}-2\frac{Ma_\infty}{a_\infty}\Phi_{xt}=0$$

with

(2) $$\Phi=\phi_0+\phi\cdot e^{i\omega t}$$

To get a fast and robust solution, several simplifications are implemented (for details see [8]), which are:

- Lifting surfaces: thickness to profile depth is small ⇒ no source distribution ⇒ flat plates
- Bodies: little lift ⇒ only source distribution and no doublet distribution ⇒ pure bodies

In addition wakes are substituted by introduction of the acceleration potential Ψ, so that there is no need to model wakes. As result equation (3) represents the influence of the structural displacements $\{\boldsymbol{h}\}$, defined at the aerodynamic boxes, on the aerodynamic forces $\{\boldsymbol{F}_h\}$.

$$\{\boldsymbol{F}_h\} = q_\infty [AIC]\{\boldsymbol{h}\} \tag{3}$$

To transfer the structural displacements $\{\boldsymbol{x}\}$ from the FE-nodes to the aerodynamic boxes a spline approach is used.

2.3.2. Fluid Structure Interaction

The fluid structure interaction in ZAERO is performed by a spline approach [8] which has to fulfil equation (4).

$$\{\boldsymbol{h}\} = [\boldsymbol{G}]\{\boldsymbol{x}\} \tag{4}$$

The spline module of ZAERO generates the spline matrix $[\boldsymbol{G}]$, in order to transfer the FE-node displacement $\{\boldsymbol{x}\}$ into a displacement $\{\boldsymbol{h}\}$ of an aerodynamic box. According to equation (4) the forces on the structural nodes $\{\boldsymbol{F}_a\}$ can be written in equation (5) as a product of the transpose the spline matrix $[\boldsymbol{G}]$ and the aerodynamic forces $\{\boldsymbol{F}_h\}$.

$$\{\boldsymbol{F}_a\} = [\boldsymbol{G}]^T\{\boldsymbol{F}_h\} \tag{5}$$

The combination of equations (3) to (5) results in equation (6) that shows the direct coherence of the AIC matrix, the structural displacements $\{\boldsymbol{x}\}$ and the resulting forces $\{\boldsymbol{F}_a\}$ on the structural nodes:

$$\{\boldsymbol{F}_a\} = q_\infty [\boldsymbol{G}]^T [\boldsymbol{AIC}][\boldsymbol{G}]\{\boldsymbol{x}\} \tag{6}$$

In the application there are different types of splines for the idealisation of the model component's movement represented by $[\boldsymbol{G}]$. The following list gives an overview of rigid coupling and the spline types that can be used with the different model component types:

- rigid type: rigid body movement with reference to movement of one structural grid point
- beam spline: translation and rotation, FE-nodes have to be along a line and have to reach to the ends of the aerodynamic plate/ body
- infinite plate spline : translation only, FE-nodes have to match up to the edges of the aerodynamic plate
- 3D volume spline: translation only, FE-nodes have to match up to the surface of the aerodynamic plate/ body and should not be in the same plane

Where the rigid type of coupling, the beam spline and the 3D volume spline can be adopted to both bodies and wing like components, the infinite plate spline is only applicable for wing like components.

2.3.3. Flutter Stability Analysis

For the solution of the basic flutter equation the g-method is applied, which was introduced by Chen in 1999 (cp. [10]). It is an extended version of the well-known pk-method (e.g. used by MSC.NASTRAN®; [8] and [11]). Both methods are based on the so-called p-method flutter equation, which reads

$$\left(\left(\frac{V}{L}\right)^2 [\boldsymbol{M}]p^2 + [\boldsymbol{K}] - q_\infty [\boldsymbol{Q}(p)]\right)\{\boldsymbol{q}\} = \{0\} \tag{7}$$

The main difference between the pk- and the g-method is the approach for the damping term in the unsteady aerodynamic term $[\boldsymbol{Q}(\mathrm{ik})]$, which replaces the transient term $[\boldsymbol{Q}(\mathrm{p})]$ in equation (7). By substituting the non-dimensional Laplace parameter

$$p = g + ik = \gamma \frac{\omega L}{V} + \frac{\omega L}{V} \tag{8}$$

and the transient aerodynamic force term

$$[\boldsymbol{Q}(p)] = [\boldsymbol{Q}^R(ik)] + [i\boldsymbol{Q}^I(ik)], \tag{9}$$

the pk-formula results from (7) with (8) and (9) as

(10)

$$\left(\left(\frac{V^2}{L^2}\right)[\boldsymbol{M}]p^2 + [\boldsymbol{K}] - q_\infty \frac{[\boldsymbol{Q}^I(ik)]}{k} p - q_\infty [\boldsymbol{Q}^R(ik)]\right)\{\boldsymbol{q}\} = \{0\}\cdot$$

For small damping terms g the unsteady aerodynamic term can be approximated by

$$[\boldsymbol{Q}(p)] \approx [\boldsymbol{Q}(ik)] + g\frac{[\partial \boldsymbol{Q}(ik)]}{\partial g}\cdot \tag{11}$$

The g-formula results from (7) with (11) to

(12)

$$\left(\left(\frac{V^2}{L^2}\right)[\boldsymbol{M}]p^2 + [\boldsymbol{K}] - q_\infty \frac{[\partial \boldsymbol{Q}(ik)]}{\partial g} g - q_\infty [\boldsymbol{Q}(ik)]\right)\{\boldsymbol{q}\} = \{0\}\cdot$$

Whereas in the pk-method the damping approach is coupled to the imaginary part of $[\boldsymbol{Q}(\mathrm{ik})]$ (i.e. $[\boldsymbol{Q}^I(\mathrm{ik})]$), the g-method uses the damping perturbation method (cp. [10]) that leads to the partial derivation of $[\boldsymbol{Q}(\mathrm{ik})]$ to g (i.e. $[\boldsymbol{Q}'(\mathrm{ik})]$) as a damping proportional term. The differences in the results are broadly discussed in [8].

3. MODELS FOR NASTRAN AND ZAERO

In this chapter the models for the MSC.NASTRAN® and ZAERO® calculation are detailed for a design abutted to a Fairchild Dornier 728 JET (FD 728JET) transport aircraft [12].

3.1. NASTRAN FE-Model

The NASTRAN model of the recalculated FD 728JET transport aircraft is shown in FIG 3. (further named PrADO 728JET). The right hand side half model consists of beam and shell elements. Additionally there are two kinds of **m**ulti **p**oint **c**onstraints (MPC) used to connect nodes/ elements. These are the **r**igid **b**oundary **e**lement type **2** (RBE2, cp. [13]) for fixed couplings (e.g. floor to skin) and the **r**igid **b**oundary **e**lement type **3** (RBE3) for interpolated displacements/ mass forces.

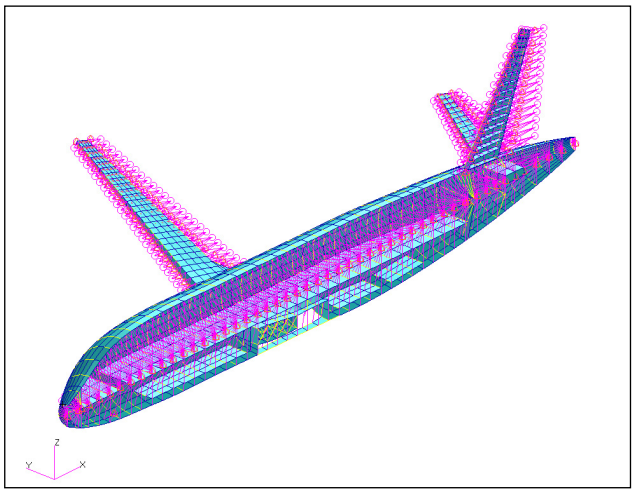

FIG 3. NASTRAN – FE-model with leading and trailing edge MPCs and condensated fuselage masses

The primary structure is represented by beams and shells and the secondary structure such as leading and trailing edge elements are modelled by **n**on **s**tructural **m**asses (NSM, e.g. flaps, fuel or galleys), connected in their centre of gravity to the primary structure (e.g. rudder of the VTP in FIG 3.) via RBE3s. Particularly in the fuselage the NSMs are condensated to the centreline of the fuselage and connected to the spars via RBE3s in respect to the spline modelling in ZAERO®. Because of the splining there are non structural nodes added, which are positioned on the leading and trailing edges of the lifting surfaces and are connected via RBE3 (e.g. trailing edge of the VTP in FIG 3.).

Furthermore, due to the use of a half model, the model is constrained at all nodes in the symmetry plane (xz-plane).

load case	constraints
symmetric	- translational in y-direction - rotational in x- and z-direction
anti symmetric	- translational in x- and z-direction - rotational in y-direction

TAB 1. FE-model constraints

TAB 1. shows the constraints for the symmetric and anti symmetric BCs related to the coordinate system in FIG 3. All other nodes are free in translation and rotation.

3.2. ZAERO® Model

3.2.1. ZAERO® Aerodynamic Model

The ZAERO® aerodynamic model can be divided into bodies and lifting surfaces or wing like components. A wake, which usually is needed by panel codes like HISSS, is not necessary as mentioned above.

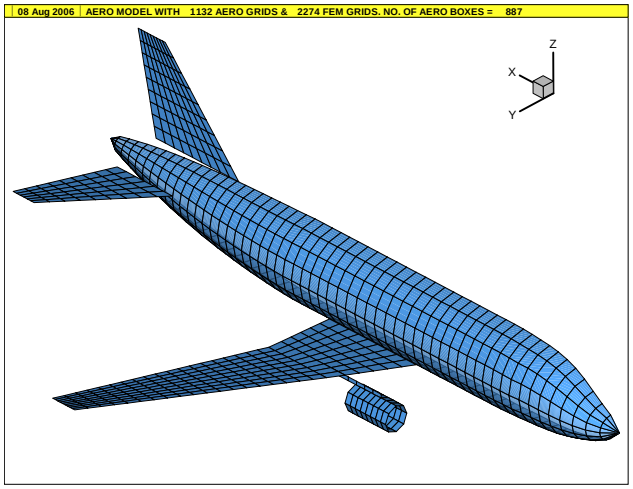

FIG 4. ZAERO® – Aerodynamic Model

FIG 4. depicts the aerodynamic right hand side half model of the PrADO 728JET transport aircraft. Besides of the fuselage all components are modelled as wing like components with so-called CAERO7 cards in the ZAERO input. While the wing is divided with respect to the dihedral into several connected CAERO7 trapezoids, the VTP and the HTP consist of a single flat CAERO7 trapezoid. Geometric twists and setting angles cannot be modelled with CAERO7 cards. The gaps between each the wing, VTP and HTP and the fuselage are filled by a so-called **v**ortex **c**arriage **t**hrough method (VCT; [7]). The pylons are represented by a single CAERO7 rectangle and nacelles are composed by eight CAERO7 rectangles.

The fuselage is modelled as a body with a single BODY7 entry. For BODY7 entries, bodies of revolution, elliptic bodies and arbitrary bodies are possible. Here an elliptic body is modelled, because it provides the best approximation with the geometry of the fuselage.

3.2.2. ZAERO Splining

The splining has to be done with a lot of care, since most errors that occur in the flutter calculation are caused by bad splines. Therefore ZAERO gives one the opportunity to check the splining by plotting the structural modes onto the aerodynamic mesh. FIG 5. gives an example of the fourth structural mode shape transferred to the aerodynamic mesh. Mode one to three are rigid modes with respect to symmetric/ anti symmetric constraints, so

that mode 4 is the first flexible mode. In this case this is the first bending mode. For the splining the fuselage is idealized as a beam spline, which is defined by the fuselage's centreline (cp. FIG 4.) and reaches from the front bulkhead to the end of the tail cone. In this way the aerodynamic boxes are well coupled to the beam spline (SPLINE2) and only little interpolation of the spline to the ends of the fuselage is necessary (cp. [6]).

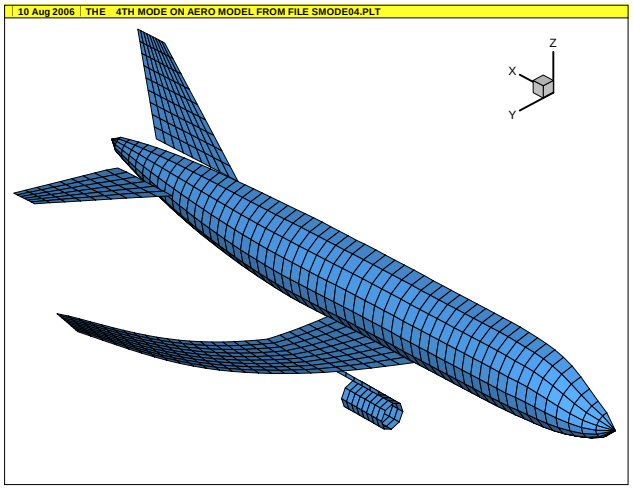

FIG 5. ZAERO – Fourth structural mode plotted on aerodynamic model

For splining the wing, and the other lifting surfaces, the **i**nfinite **p**late **s**pline (IPS, SPLINE1) produces the best results. For the spline definition the leading and trailing edge nodes (cp. FIG 3.) are used. To realize a smooth gradient of the spline in respect to the lifting surface fuselage connection, the centre nodes of the fuselage with the matching x-position are added to the lifting surface spline definition. In a similar way, the pylon connection to the wing is implemented. Besides, the wing is built up from different CAERO7 trapezoids, the spline definition of a single CAERO7 card contains all nodes of the wing and fuselage. This has to be done, because only in this way a smooth deflection gradient for the whole wing can be guaranteed. The single nacelle lifting surfaces are firmly attached to the centre of gravity node of the power plant by an ATTACH entry (cp. [7]).

The smooth gradients in the component deflection are needed for the calculation of the unsteady aerodynamics. Gaps or bumps in the CAERO7 deflection would lead to error afflicted results and have to be avoided.

4. RESULTS OF THE RECALCULATED FD 728JET

4.1. Baseline Aircraft Characteristics

In TAB 2. the aircraft characteristics from the original FD 728JET [12] and data recalculated with PrADO are compared. It is observable that the error in per cent of the examined values is lower than six per cent. This reflects the accuracy of PrADO for general aircraft properties. For details like the stiffness distribution of the structure or the real mass distribution no data for comparison are available, which would be helpful to evaluate differences in the modal analysis.

Aircraft Design Characteristics					
Value	**Abbr.**	**Unit**	**FD 728JET**	**PrADO 728JET**	**Error in %**
Span	B	m	27.12	27.12	0.00%
Length	L	m	27.04	26.65	-1.46%
Height	H	m	9.05	9.35	3.21%
Thrust	S	kN	2x55.6	2x55.6	0.00%
Operating Empty Weight	OEW	kg	21489	22113	2.82%
Max. Fuel Weight	MFW	kg	10184	10006	-1.78%
Max. Payload	-	kg	8811	9363	5.90%
Max. Take Off Weight	MTOW	kg	35200	34746	-1.31%
Max. Landing Weight	MLW	kg	32420	32914	1.50%

TAB 2. Summary of the aircraft characteristics (cp. [12])

However, the preliminary design raises no claim to calculate absolute results, but brings out trends between variants, which are calculated with the same methods. On the basis of the flutter results, shown below, this aspect is to be detailed.

4.2. Modal Analysis Results of the PrADO 728JET Baseline Design

In TAB 3. the results of the modal analyses with MSC.NASTRAN® for the PrADO 728JET with OEW and a typical flight condition are shown for symmetric and anti symmetric BCs. In comparison the results from a FD 728JET also for the typical flight case is given (cp. [1]). The numbering of modes of FD 728JET and PrADO 728JET is different, because the PrADO model is a half model and therefore for every BC there are three rigid modes (mode 1 to 3). Instead in the full FD 728JET model the first six modes are rigid modes (mode 1 to 6). So, for the comparison in TAB 3. the same eigen shapes are contrasted in respect to their frequencies for the first twelve modes. It can be seen that most shapes and frequencies are in good compliance but for some frequencies no matching shape can be found.

Results of the Modal Analyses								
Configuration								
FD 728JET			PrADO 728JET baseline					
Mass			Mass			Mass		
design mission			OEW			design mission		
nr.	BC	ω in Hz	nr.	BC	ω in Hz	nr.	BC	ω in Hz
7	s	2.649	4	s	2.850	4	s	2.788
8	a	3.704	5	a	3.832	5	a	3.736
11	a	5.567	6	a	5.615	6	a	5.103
14	a	6.700	8	a	7.088	8	a	6.950
15	s	7.370	5	s	7.406	5	s	6.878
16	a	7.466	9	a	7.439	-	-	-
17	s	7.989	6	s	7.631	6	s	7.501
18	a	8.054	-	-	-	10	a	8.703
19	s	9.190	7	s	8.777	8	s	9.200
20	a	9.526	10	a	9.676	11	a	9.719
21	s	10.093	9	s	10.082	10	s	9.777
22	a	10.353	12	a	10.159	13	a	10.734
s=symmetric; a = anti symmetric								

TAB 3. Extract of the eigen frequencies (cp. [1])

The differences in the eigen frequencies for the PrADO 728JET and the FD 728JET can partially be explained by the differences in the set up of the dynamic model. The FD 728JET dynamic model contains more details (e.g. control surfaces).

Furthermore sizing method in PrADO (cp. [5]) is primarily coded for component mass calculation. This causes an inaccuracy in the stiffness distribution, which is normally not only driven by critical stresses. In summary it can be stated that the basic mode shapes are in good compliance.

4.3. Results of the Flutter Calculation

The flutter calculation with ZAERO is performed for the design mission: velocity range from 0 to 400m/s (Ma=0.85 as reference speed for the instationory aerodynamic, non matched point flutter calculation) at H=6800m (ρ=0.6024kg/m³) with 3800kg payload and 6200kg fuel. It has to be proven that the critical flutter speeds are above $1.15V_{EAS}$. Consequently V_{TAS} is 313,1m/s (cp. [1],[14]). As one result FIG 6. shows the frequency-velocity and the damping-velocity diagram for symmetric boundary conditions and structural damping assumed zero. The damping curves for all modes do not cross the zero damping axis and so the system is stable. For this flight condition and in the examined velocity range the configuration is free of flutter. This is also valid for the anti symmetric BC (result summary cp. TAB A.1).

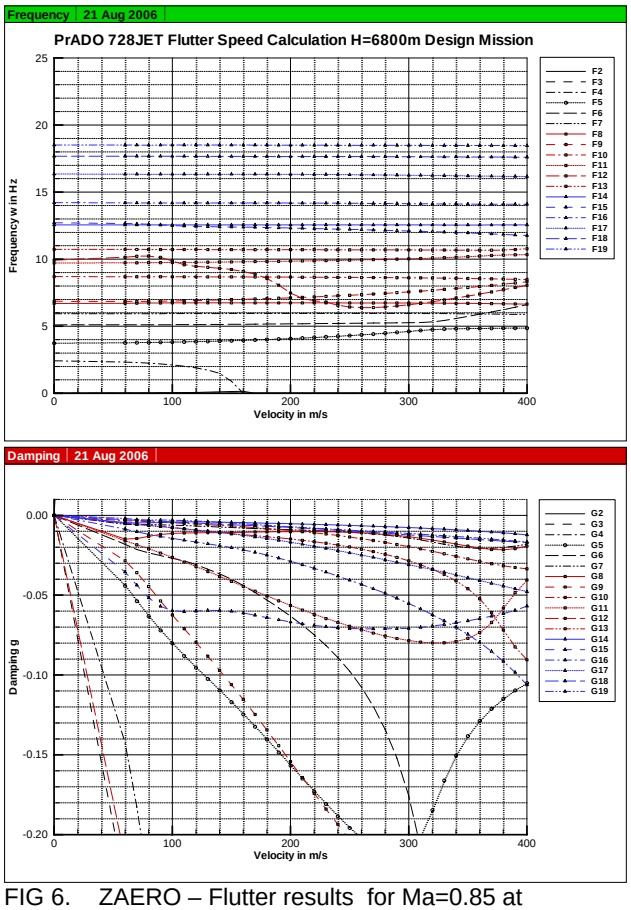

FIG 6. ZAERO – Flutter results for Ma=0.85 at H=6800m with sym. BC of PrADO 728JET

In reference [1] it is shown that the FD 728JET model has in contrast a first critical flutter speed at V=388m/s produced by the HTP bending coupled with the elevator deflection. The absence of this flutter mode in the flutter calculation of the PrADO 728JET is caused by the non-existence of control surfaces in the PrADO structural model. In [1] further critical flutter speeds are found above 400m/s. Only one case should be mentioned here, because mode seven of FD 728JET gets critical at 405m/s. This flutter mode is caused by the first wing bending shape and interacts with the power plant/ wing torsion mode. In the next chapter it is evinced that these cases can be predicted by the PrADO process also.

5. COMPARISON OF VARIANTS

A PrADO 728JET modification (PrADO 728JET WL) with winglets is designed to examine the influence of winglets on the flutter stability and to show the functionality of the process. In TAB 4. the basic data for this PrADO 728JET design with winglets are summarised. It is treated as a new design and has passed through the complete PrADO design process. That means that the influence of steady aerodynamic loads induced by the winglet is considered in the sizing of all components and also the interaction of the other aircraft parameters are regarded.

Aircraft Design Characteristics					
Value	Abbr.	Unit	PrADO 728JET	PrADO 728JET WL	Dif. in %
Span	B	m	27.12	27.12	0.00%
Length	L	m	26.65	26.65	0.00%
Height	H	m	9.35	9.35	0.00%
Thrust	S	kN	2x55.6	2x55.6	0.00%
Operating Empty Weight	OEW	kg	22113	22436	1.44%
Mission Fuel Weight	-	kg	6123	6105	-0.29%
Max. Payload	-	kg	9363	9363	0.00%
Max. Take Off Weight	MTOW	kg	34746	35051	0.87%
Max. Landing Weight	MLW	kg	32914	33229	0.95%

TAB 4. Comparison of variant to baseline characteristics

The motivation for installing a winglet is normally to improve the aerodynamic performance for the design mission, so that the aircraft is more economical. The PrADO 728 JET WL variant has a 1% better lift to drag ratio for the design flight mission. The impacts on the flutter stability for the same flight condition as before are shown in FIG 7. The modified design has a first critical flutter speed for symmetric boundary conditions at V=373,67m/s and is therefore higher than the allowable speed (V_{TAS} =313.1m/s).

As it can be seen in FIG 7. the first flutter mode is caused by the 8th symmetric structural mode. The 8th mode shape is figured in FIG A.2 and the corresponding flutter mode shapes in FIG A.3. Furthermore it can be seen that the frequencies of mode 5 and mode 8 approach near each other with increasing speed. Also, while the damping gets more stable for mode 5, in the same way the damping of mode 8 becomes critical. In comparison the characteristic of the two mode shapes (mode 5 cp. FIG A.1 and mode 8) are very similar, so the energy transfer from mode 5 to 8 can be understood.

The flutter results for the anti symmetric BC are summarized in TAB A.1. The critical speed therefore is V=342.41m/s (cp. FIG A.4) ,which is also above the

limit. Thus the influence of a winglet significantly decreases the critical flutter speed, but the lowest flutter speed is still above the mandatory limit.

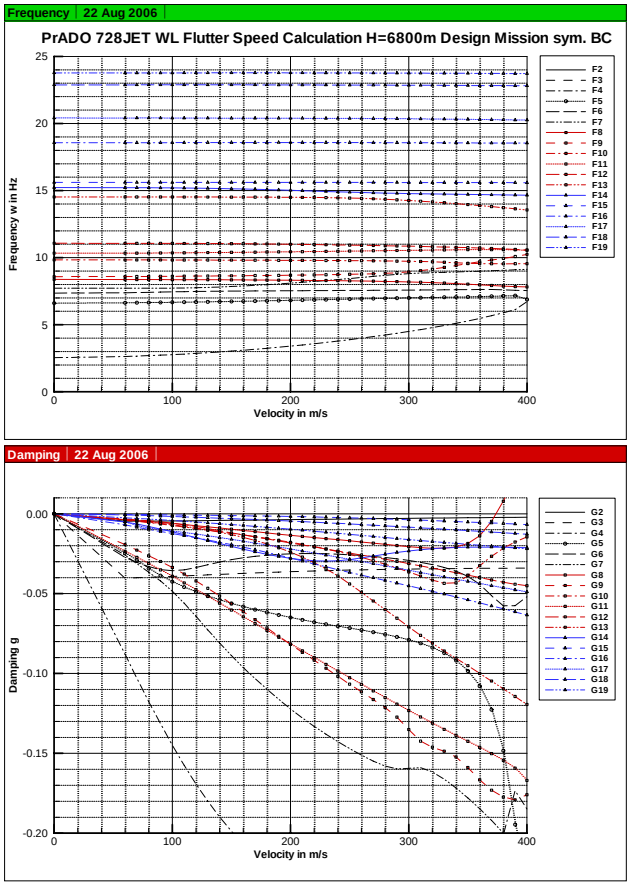

FIG 7. ZAERO – Flutter results for Ma=0.85 at H=6800m with sym. BC of PrADO 728JET WL

6. CONCLUSION

The methodology of the preliminary aircraft design tool PrADO have been expanded by the functionality to analyse the aeroelastic stability by predicting critical flutter speeds. Therefore a process has been installed, which is based on validated programs.

One uncertainty in the flutter speed prediction is caused by the structural sizing method, which generates stiffness and mass distributions with small deviations compared to the industrial design process. This fact must be accepted in the preliminary design phase. But regarding this fact, the presented flutter results for two different aircraft configurations show correct tendencies of change in critical flutter speeds. Further it has been shown that the process cannot predict the impact of control surfaces on flutter speeds, which are thereby induced. In this place it would be advantageous to improve the method by integrating control surfaces into the FE and aerodynamic model, so that more precise predictions can be made.

Summarising, it can be stated, that the process is capable of predicting flutter cases in the preliminary design phase. Therefore this process gives the advantage of the ability to perform parametric designs analyses in order to find a flutter free design.

7. REFERENCES

[1] Riedel, S., “MSC/NASTRAN-ZAERO, ein Vergleich kommerzieller Software zur Berechnung des Flatterverhaltens am Beispiel der 728JET”, Diploma Thesis University of Applied Sciences Hamburg, Fachbereich Fahrzeugtechnik und Flugzeugbau, 2002

[2] Heinze, W., “Ein Beitrag zur quantitativen Analyse der technischen und wirtschaftlichen Auslegungsgrenzen verschiedener Flugzeugkonzepte für den Transport großer Nutzlasten”, PhD-Thesis TU Braunschweig, ZLR Forschungsbericht 94-01, 1994

[3] Horstmann, K-H., “Ein Mehrfach-Traglinienverfahren und seine Verwendung für Entwurf und Nachrechnung nichtplanarer Flügelanordnungen“, PhD-Thesis TU Braunschweig, DFVLR-Forschungsbericht 87-59, 1987

[4] Fornasier, L., “A Higher-Order Subsonic/Supersonic Singularity Method for Calculating Linearized Potential Flow”, 23rd Aerospace Science Meeting & Ehibit, Reno, AIAA 84-1646, 1984

[5] Österheld, C., “Pysikalisch begründete Analyseverfahren im integrierten multidisziplinären Flugzeugentwurf”, PhD-Thesis TU Braunschweig, ZLR Forschungsbericht 2003-06, 2003

[6] Piegel, L., Tiller, W., “The NURBS Book”, Springer Verlag Berlin, 1997

[7] NN, “ZAERO Version 7.3: Users Manual”, ZONA 02-12.1, ZONA Technology Inc., 2005

[8] NN, “ZAERO Version 7.3: Theoretical Manual”, ZONA 02-12.4, ZONA Technology Inc., 2005

[9] Theodorsen, T., ”General Theory of Aerodynamic Instability and Mechanism of Flutter”, NACA Report 496, 1935

[10] Chen, P.C., ”A damping perturbation method for flutter solution: the g-method”, AIAA Journal Vol. 38, No. 9, Sep 2000, pp. 1519-1524

[11] NN.,”MSC.NASTRAN Aeroelastic Analysis Users’ Guide V68”, MSC Software Corporation, 2004

[12] Bansa, F., “Flugzeugentwurf am Beispiel einer Fairchild Dornier 728JET”, Thesis University of Applied Sciences Hamburg, Fachbereich Fahrzeugtechnik und Flugzeugbau, 2003

[13] NN.,”MSC.NASTRAN Quick Reference Guide”, MSC Software Corporation, 2005

[14] NN., “Certification Specifications for Large Aeroplanes: CS-25”, European Aviation Safety Agency - EASA, 17.10.2003; http://www.easa.eu.int/home/certspecs_en.html

8. ACKNOWLEDGMENTS

Part of the work is funded by the German aerospace research program (LuFo3) during the project MODYAS (Multi Objective Dynamic Aircraft Synthesis; managed by M. Kordt).
Thanks is extended to L. Fornasier/ EADS-M for providing the HISSS panel code.

9. ANNEX

		Configuration			
		PrADO 728JET		PrADO 728JET WL	
altitude	BC	OEW	design mission	OEW	design mission
0m	sym.	- V_c=365.86m/s at mode 10 - V_c=386.90m/s at mode 8	- V_c=338.80m/s at mode 8	- V_c=277.23m/s at mode 8 - V_c=320.80m/s at mode 11 - V_c=335.49m/s at mode 9	- V_c=267.70m/s at mode 8 - Vc=353.03m/s at mode 12
	anti sym.	- V_c=376.17m/s at mode 12 - V_c=384.89m/s at mode 9	- V_c=368.37m/s at mode 15	- V_c=257.93m/s at mode 9 - V_c=305.75m/s at mode 10	- V_c=255.38m/s at mode 8
6800m	sym.	no flutter	no flutter	- V_c=393.83m/s at mode 8 - V_c=396.81m/s at mode 5	- V_c=373.67m/s at mode 8
	anti sym.	no flutter	no flutter	- V_c=350.36m/s at mode 9	- V_c=342.41m/s at mode 8
12015m	sym.	no flutter	no flutter	no flutter	no flutter
	anti sym.	no flutter	no flutter	no flutter	no flutter

TAB A.1 Summary of flutter calculation results

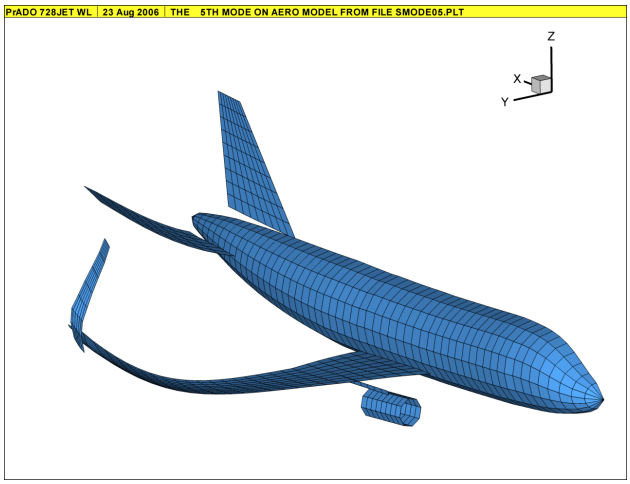

FIG A.1 ZAERO – Plotted structural mode 5 on the aerodynamic mesh (sym. BC)

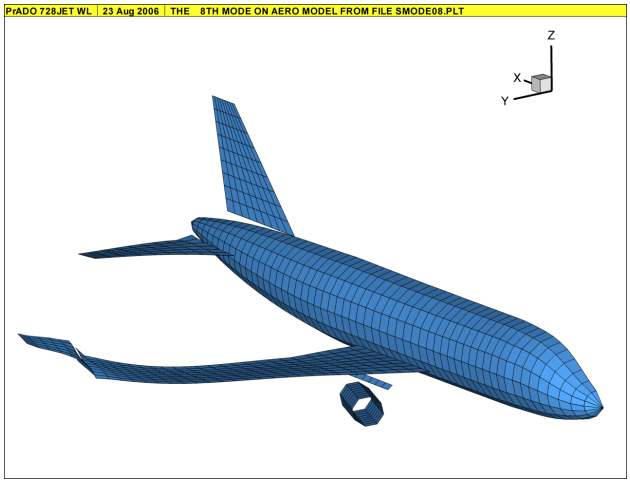

FIG A.2 ZAERO – Plotted structural mode 8 on the aerodynamic mesh (sym. BC)

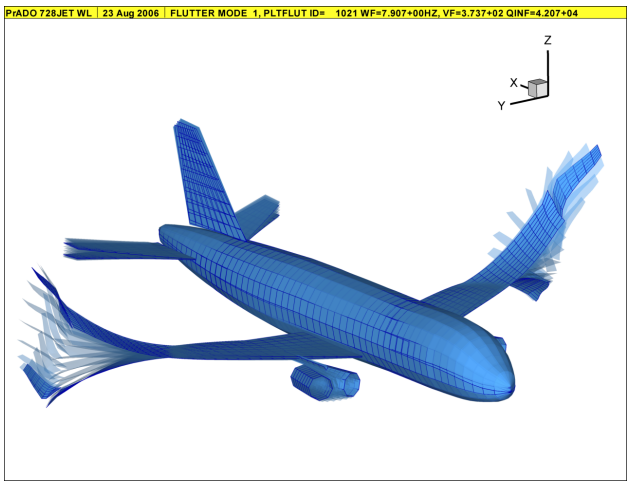

FIG A.3 ZAERO – Flutter mode 1 at 373.67m/s at with sym. BC of PrADO 728JET WL

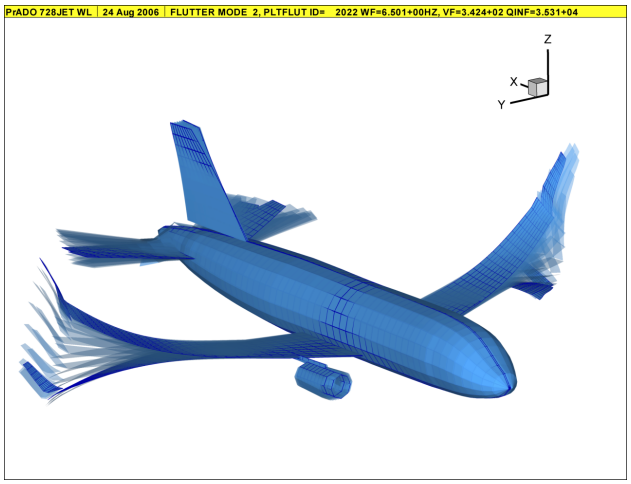

FIG A.4 ZAERO – Flutter mode 1 at 342.41m/s at with anti sym. BC of PrADO 728JET WL